Secondary Structure of the Third Extracellular Loop Responsible for Ligand Selectivity of a Mammalian Gonadotropin-Releasing Hormone Receptor

Renate Petry,[†] David Craik,[‡] Gerald Haaima,[‡] Bernhard Fromme,[§] Horst Klump,[||] Wolfgang Kiefer,*[,†] Dieter Palm,[⊥] and Robert Millar[#,§]

Institut für Physikalische Chemie, Universität Würzburg, Am Hubland, D-97074 Würzburg, Germany, Institute for Molecular Bioscience, The University of Queensland, Brisbane, QLD 4072, Australia, Department of Medical Biochemistry, University of Cape Town, Observatory 7425, South Africa, Department of Molecular and Cellular Biology, University of Cape Town, Private Bag, Rondebosch 7701, South Africa, Theodor-Boveri-Institut für Biowissenschaften, Physiologische Chemie I, Universität Würzburg, Am Hubland, D-97074 Würzburg, Germany, and Human Reproductive Sciences Unit, 37 Chalmers Street, Edinburgh EH3 9ET, Scotland, U.K.

Received September 6, 2001

The extracellular loop 3 (ECL3) of the mammalian gonadotropin-releasing hormone receptor (GnRH-R) contains an acidic amino acid (Glu^{301} in the mouse GnRH-R) that confers agonist selectivity for Arg^8 in mammalian GnRH. It is proposed that a specific conformation of ECL3 is necessary to orientate the carboxyl side chain of the acidic residue for interaction with Arg^8 of GnRH, which is supported by decreased affinity for Arg^8 GnRH but not Gln^8 GnRH when an adjacent Pro is mutated to Ala. To probe the structural contribution of the loop domain to the proposed presentation of the carboxyl side chain, we synthesized a model peptide (CG*PEMLNRVSEP*GC) representing residues 293−302 of mouse ECL3, where Cys and Gly residues are added symmetrically at the N and C termini, respectively, allowing the introduction of a disulfide bridge to simulate the distances at which the ECL3 is tethered to the transmembrane domains 6 and 7 of the receptor. The ability of the ECL3 peptide to bind GnRH with low affinity was demonstrated by its inhibition of GnRH stimulation of inositol phosphate production in cells expressing the GnRH-R. The CD bands of the ECL3 peptides exhibited a superposition of predominantly unordered structure and partial contributions from β-sheet structure. Likewise, the analysis of the amide I and amide III bands from micro-Raman and FT Raman experiments revealed mainly unordered conformations of the cyclic and of the linear peptide. NMR data demonstrated the presence of a β-hairpin among an ensemble of largely disordered structures in the cyclic peptide. The location of the turn linking the two strands of the hairpin was assigned to the three central residues L^{296}, N^{297}, and R^{298}. A small population of structured species among an ensemble of predominantly random coil conformation suggests that the unliganded receptor represents a variety of structural conformers, some of which have the potential to make contacts with the ligand. We propose a mechanism of receptor activation whereby binding of the agonist to the inactive receptor state induces and stabilizes a particular structural state of the loop domain, leading to further conformational rearrangements across the transmembrane domain and signal propagating interaction with G proteins. Interaction of the Glu^{301} of the receptor with Arg^8 of GnRH induces a folded configuration of the ligand. Our proposal thus suggests that conformational changes of both ligand and receptor result from this interaction.

Introduction

Gonadotropin-releasing hormone (GnRH), a hypothalamic decapeptide (pGlu-His-Trp-Ser-Tyr-Gly-Leu-Arg-Pro-Gly-NH_2), is the primary regulator of reproductive function. It interacts with high-affinity receptors on pituitary gonadotrope cells to stimulate the biosynthesis and pulsatile release of luteinizing hormone and follicle-stimulating hormone and ultimately steroidogenesis and gametogenesis.[1]

The GnRH receptor is a member of the rhodopsin-like G-protein-coupled receptor (GPCR) family[2] with seven hydrophobic (α-helical) transmembrane domains (TMD) connected by extracellular and intracellular loops.[2,3] It is one of the smallest GPCRs (Figure 1), containing 327 amino acids in rodent receptors and 328 amino acids in other mammalian receptors.[2] Molecular models of the GPCR family have been based on structural data obtained from X-ray crystallography of bacteriorhodopsin[6] and of bovine rhodopsin.[7] Although the transmembrane domains of related GPCRs can be modeled by analogy because of the high level of homology, the structure of the loops and N or C termini cannot be predicted on homology alone because of their large

* To whom correspondence should be addressed. Phone: +49-931-888 6330. Fax: +49-931-888 6332. E-mail: wolfgang.kiefer@mail.uni-wuerzburg.de.
[†] Institut für Physikalische Chemie, Universität Würzburg.
[‡] The University of Queensland.
[§] Department of Medical Biochemistry, University of Cape Town.
[||] Department of Biochemistry, University of Cape Town.
[⊥] Theodor-Boveri-Institut für Biowissenschaften, Physiologische Chemie I, Universität Würzburg.
[#] Human Reproductive Sciences Unit.

10.1021/jm011036k CCC: $22.00
Published on Web 02/05/2002

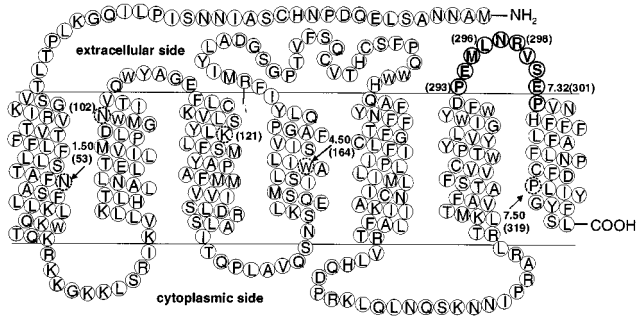

Figure 1. Primary sequence and proposed topology of the mouse GnRH receptor. The residues of the third extracellular loop (ECL3) are shown in bold typeface. The consensus numbering scheme facilitates the comparison of equivalent amino acid residues in the different rhodopsin-like GPCRs.[4,5] The most conserved residue in a TMD is assigned the number 50, to which neighboring amino acids in the same TMD are numbered. Amino acids positioned toward the N terminus of this conserved locus have numbers descending from 50, and residues toward the C terminus of the TMD have numbers increasing from 50. The number identifying the TMD precedes this number. For example, in helix 7 of the mouse GnRH-R, the most conserved residue is Pro in position 319 and is designated the number 50 ($Pro^{7.50(319)}$). Glu^{301} is found in the extracellular portion of TM7 and is 18 amino acids away from $Pro^{7.50}$ toward the N terminus and is therefore designated the number 7.32 ($Glu^{7.32(301)}$). In the human GnRH-R this residue is $Asp^{7.32(302)}$.

variation in length and composition. However, 2D NMR spectroscopy of peptides representing all extramembraneous regions of rhodopsin showed that peptides corresponding to loop domains in rhodopsin formed loops in solution and displayed the same secondary structure as found in the structure of the intact protein.[8−10] The structure of rhodopsin disclosed highly organized extramembraneous regions, which act structurally and biologically as protein domains.[10,11] This gives confidence in assessing the loop structures and functions of related GPCRs by assembling data from corresponding peptides.[12] Structural information on the transmembrane domains and the loops can be pieced together to generate a molecular model of rhodopsin and related GPCRs including the GnRH-R that allows prediction of how GnRH binds and activates its receptor.[8,9]

The high degree of conservation among the rhodopsin-type GPCRs suggests that members of this family of receptors share a common structural framework and mechanism of activation. Receptor activation by agonists at the extracellular face is associated with conformational changes in the membrane that facilitate signal-propagating interactions at the intracellular face.[13,14] For GPCRs, the active conformation is related to a ternary complex consisting of hormone, receptor, and G protein. This model includes an initial binding step, common to both agonists and antagonists and hence not restrictively discriminating between ligands, followed by a transition step exclusive to agonists.[14] Since receptor activation is initiated by binding of an agonist ligand, the conformational changes associated with receptor activation must have their origin in the ligand binding pocket.

It was proposed that GnRH agonist binding involves residues in TM3 (Lys^{121}) and at the N-terminal end of TM2 (Asp^{98} and Asn^{102}).[15−17] In addition to residues in the transmembrane domains, the extracellular loop three (ECL3) has been implicated in binding GnRH.[2,14,18,19] In ECL3 a conserved acidic residue ($Glu^{7.32(301)}$ in the mouse receptor, $Asp^{7.32(302)}$ in the human receptor) interacts with Arg^{8} in GnRH.[18,19] GnRH may be induced to assume a "high-affinity" conformation by an interaction that involves the Arg^{8} and the Glu^{301} receptor residue.[18] This raises the question as to what extent the conformation of the ECL3 domain contributes to the "high-affinity" binding state of the GnRH-R. One contribution might come from a Pro residue following $Glu^{7.32}$/$Asp^{7.32}$ (Figure 1). Mutation of Pro to Ala decreases affinity for Arg^{8} GnRH but not Arg^{8}-substituted GnRHs (B. Fromme, unpublished results). Proline confers unique local constraints on peptide chain conformation because the α-nitrogen atom of proline is part of the rigid pyrrolidine ring, and by means of a secondary amide bond, it is covalently bound to the preceding amino group.[20] Possibly the EP/DP motif in mouse/human GnRH-R supports efficient interaction of the electrostatic potential between E or D and Arg^{8} of GnRH by the preferred orientation of the acidic side chain. In addition, it was proposed that the secondary structure of the loop domain might play a role for ligand recognition and consecutive activation of the receptor.[19]

Structural characterization of the extracellular functional domains by synthetic peptides modeled to mimic the native loop structure has been successfully applied to the human thromboxane A_2[21] and rhodopsin receptors.[8−10] Essentials of the structural information were acquired by circular dichroism and the 2D NMR technique. This paper utilizes these same techniques and describes a comparative investigation of a loop peptide, extending the technical approach to Raman spectroscopy. To mimic the third extracellular domain, we synthesized a peptide representing residues 293−302 of mouse ECL3 and added Cys and Gly residues symmetrically at the N and C termini, allowing the introduction of a disulfide bridge to simulate a looplike constrained form as is present in the native receptor in which it is attached to TM6 and TM7.

Materials and Methods

Peptide Synthesis. The peptide designed for this investigation is a 14mer with the sequence C*GPEMLNRVSEP*GC. It corresponds to residues 293−302 of the third extracellular loop of mouse GnRH-R and was synthesized by conventional solid-phase peptide synthesis using t-Boc chemistry. The linear peptide was cleaved from the resin using HF (10% cresol) and purified using reversed-phase HPLC on a C18 column. The disulfide bond in the cyclic peptide was produced by air oxidation (1:1 DMF/H_2O) of the linear peptide for 12 h, followed by HPLC purification. Mass spectrometry (MALDI-TOF) using 2,5-dihydroxybenzoic acid as a standard matrix was performed and confirmed the calculated molecular weight of the cyclic and of the linear peptide.

Phosphatidyl Inositol (PI) Hydrolysis and Inhibition of GnRH-Stimulated Phosphate Accumulation with ECL3 Peptides. COS-1 cells (2×10^5 cells/well), which were transiently transfected with the human GnRH-R, were incubated with *myo*-[2-^{3}H]inositol (1 μCi/well, Amersham, Arlington Heights, England) as previously described.[22] The labeled cells were incubated with 10^{-10} M of GnRH for 1 h at 37 °C in the presence of LiCl. Alternatively, various concentrations of ECL3 peptides or peptide controls (10^{-7}−10^{-4} M) were incubated with 10^{-10} M GnRH for 2 h at 37 °C before adding to the labeled cells. After 1 h the incubation was terminated by addition of 10 mM formic acid (1 mL/well). Inositol phosphates

(IP) were separated from the formic acid extract on DOWEX-1 ion exchange columns and eluted into scintillation liquid, and the radioactivity was counted. The ability of the ECL3 peptides to inhibit GnRH-stimulated IP production was compared to the potency of GnRH alone. IP assays were performed twice in duplicate.

Data Reduction. IP assays were performed twice in duplicate. Four−parameter nonlinear curve fitting was used to estimate the peptide concentrations required to stimulate half-maximal IP production (EC_{50}). Statistical analysis of the data consisted of an unpaired, two−tailed T test.

Spectroscopic Methods. CD spectra were recorded at room temperature on a JASCO J-720 spectropolarimeter using quartz cuvettes of 0.2 or 0.1 cm path length. Ellipticity is reported as mean residue ellipticity [Θ] in deg cm^2/dmol obtained within the range from 280 to 195 nm, representing each the average of 20 accumulated scans. CD spectroscopy was performed in two different buffers as described in Results. The concentrations of the peptide solutions were ∼500 μM in buffer I and ∼100 μM in buffer II.

NMR spectra were recorded on Bruker 500 and 750 MHz DRX spectrometers for solutions of both the cyclic and the linear peptide at temperatures in the range 280−310 K. All spectra were acquired in phase-sensitive mode using TPPI.[23] The following homonuclear spectra were recorded: double-quantum-filtered (DQF) COSY,[24] TOCSY,[25] with an MLEV17 isotropic mixing period of 80 ms,[26] and NOESY with mixing times of 200, 250, and 300 ms.[27] For the DQF-COSY experiment, the water proton signal was suppressed by lower power irradiation during the relaxation delay (1.8 s). Solvent suppression in TOCSY and NOESY experiments was achieved using a modified WATERGATE sequence[28] in which two gradient pulses of 1 ms duration and 6 G cm^{-1} strength were applied on either side of the binomial pulse. The 2D spectra were collected over 4096 data points in the F_2 dimension and 512 increments in the F_1 dimension over a spectral width corresponding to 11 ppm. All NMR spectra were processed on a Silicon Graphics workstation using XwinNMR (Bruker). The F_1 dimension was generally zero-filled to 2048 real data points with the F_1 and F_2 dimensions being multiplied by a sine-squared function shifted by 90° prior to Fourier transformation.

For the recording of the Raman spectra from lyophilized samples, a micro-Raman setup was employed using the 514 nm line of a continuous-wave argon ion laser (Spectra Physics, model 166) for excitation. The scattered light was collected in backscattering geometry by focusing a ×80 objective (Olympus ULWD MSPlan80/0.75) on the entrance slit of a SPEX 1404 0.85 m double spectrometer, which provided a spectral resolution of ∼3 cm^{-1}. The laser power at the focus spot on the sample was kept below ca. 22 mW. The detection system consisted of a nitrogen-cooled charge-coupled detector (CCD, SDS 9000 Photometrics). The acquisition of a single spectrum typically took about 6 h in the multichannel scanning technique, and four repeats on each sample were done. Collected spectra were consistent after repeated scans, and it was assumed that the conformation of the peptides was unaffected by the long exposure to the laser beam.

On a different micro-Raman instrument (LabRam, Jobin Yvon), we employed excitation by an argon ion laser (514 nm) with a laser power of ∼8 mW at the sample and a spectral resolution of approximately 5 cm^{-1}. We used a ×100 objective, 100 μm slit width, and 1800 grooves/mm diffraction grating. Each spectrum is the result of 40 accumulations with 100 s integration time.

Near-infrared Fourier transform (FT) Raman spectra were recorded on a Bruker IFS 120HS spectrometer equipped with a CaF_2 beam splitter, a FRA-106 Raman module, and a cryogenically cooled Ge detector. The excitation source was a diode-pumped Nd:YAG laser operating at 1064 nm. Scans were obtained at a resolution of 2 cm^{-1} within an overall scanning time of about 8 h to obtain acceptable signal-to-noise ratios in the spectra. Collected data were obtained in 180° backscattering geometry by exposure of lyophilized peptide sample to a laser output power of about 350 mW. No indication of photodecomposition was observed for extended periods of laser irradiation.

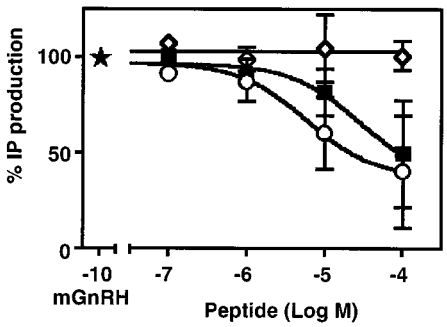

Figure 2. Inhibition of GnRH-stimulated IP production by ECL3 peptides. ECL3 peptides (10^{-7}−10^{-4} M) were preincubated with 10^{-10} M GnRH for 1 h before stimulating COS-1 cells transiently transfected with the wild-type human GnRH receptor: (■) linear ECL3 peptide and (○) cyclic ECL3 peptide. Somatostatin (◇) was used as a control. Data are mean ± SEM of two experiments, each point performed in duplicate and expressed as percentage IP accumulation relative to 10^{-10} M GnRH (∗) that was incubated alone over the same period of time.

Results

Inhibition of GnRH Stimulated PI Hydrolysis by ECL3 Peptides. We found that the linear and cyclic ECL3 peptides inhibit GnRH-stimulated IP accumulation of which the disulfide-bridged ECL3 peptide appeared to be slightly more effective in decreasing GnRH potency (Figure 2). A concentration of 10^{-4} M was needed to attain >50% inhibition of the signal. High concentrations of synthetic peptides are generally needed when the binding site or binding subsite represented by the synthetic peptide makes up only part of the "binding pocket".[12] (For illustration of the "binding pocket" of the GnRH-R, see Figure 9.) A peptide of comparable size (somatostatin, 14 amino acids) served as a check for unspecific effects at these high peptide concentrations. No unspecific effects were observed up to 10^{-4} M somatostatin. This suggests that the peptides representing ECL3 specifically compete with the receptor loop for binding of GnRH and act biologically as structural domains similar to short peptides representing intradiscal loops of rhodopsin.[8]

CD Spectroscopy. The CD spectra of the cyclic ECL3 peptide and of the linear ECL3 peptide were obtained in two different buffers (I and II) in which TFE and DTT were added consecutively (parts A and B of Figure 3, respectively). Buffer I was a standard saline buffer supplemented by inorganic salts. Since this physiological buffer was predominately used in the pharmacological characterization of a series of mutations in ECL3 or substitutions in GnRH,[18] we first have recorded the structure of the synthetic peptides in buffer I (Figure 3A). However, buffer I was strongly absorbing in the far UV range and the CD spectra had to be truncated at 207 nm, thus causing a considerable loss of information content. After addition of 1 μL of a 10-fold molar excess of DTT to the peptide solution to reduce the disulfide-bridged cyclic peptide, the CD absorption bands increased slightly. Both spectra in Figure 3A are characterized by the overall negative

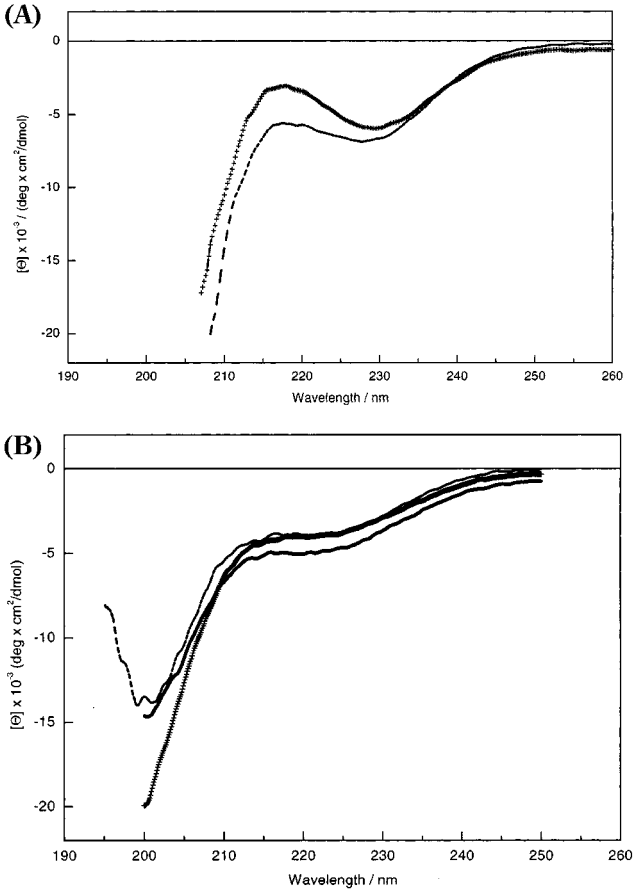

Figure 3. (A) CD spectra of ECL3 of mouse GnRH-R in buffer I at pH 7.0 (see text for details). Peptide concentration was ~500 μM, cuvette had 0.1 cm path length, + + + represents the cyclic form, and − − − represents the linear peptide obtained from the cyclic peptide by adding a 10-fold molar excess of DTT. (B) CD spectra of ECL3 of mouse GnRH-R in buffer II at pH 7.0 (see text for details) in the presence of 40% TFE and of DTT. Concentration of the peptide was ~100 μM, cuvette had 0.2 cm path length, + + + represents the cyclic form, − represents that in 40% TFE, and − − − represents the linear peptide in 40% TFE obtained from the cyclic peptide by adding a 10-fold molar excess of DTT.

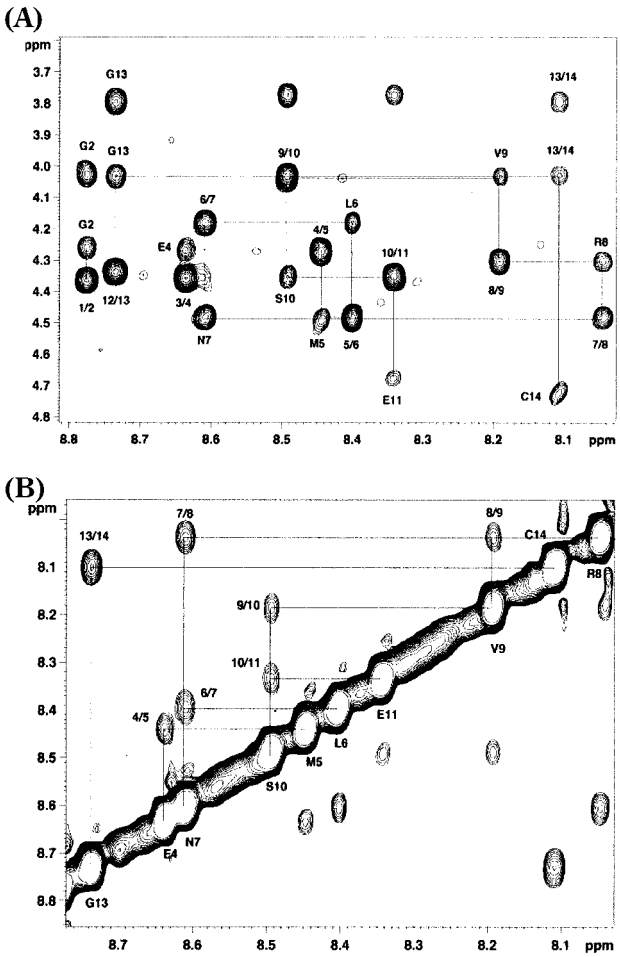

Figure 4. (A) Regions of the 750 MHz NOESY spectrum of the cyclic ECL3 peptide recorded at 280 K in aqueous solution. The fingerprint region shows sequential connectivities between residues. Intraresidue cross-peaks are indicated with the residue number, and one-letter amino acid codes and sequential NOEs are indicated by the numbers of the sequential residues. (B) Regions of the 750 MHz NOESY spectrum of the cyclic ECL3 peptide recorded at 280 K in aqueous solution. The NH−NH region shows NOEs between adjacent amide protons.

signal with a shape typically associated with random-coiled polypeptides.[29]

We then used buffer II in order to obtain spectra below 200 nm and to compensate for some of the increased absorbance due to the addition of DTT. The buffer consisted of 1 mM each of sodium citrate, sodium borate, and sodium phosphate and contained 0.1 M sodium fluoride. The overall shape of the CD spectra was not significantly different in both of the buffers used (see Figure 3). In the presence of TFE (Figure 3B) the peptide did not reveal any significant tendency to adopt helical conformation. In a 10-fold molar excess of DTT, where the disulfide bond between the flanking cysteine residues is completely reduced, the negative band near 198 nm decreased. Thus, we have assumed that β-sheet conformation partly contributes to the CD signal of the linear ECL3 peptide.

NMR Spectroscopy. The 2D NMR spectra were assigned using the standard sequential assignment procedure[30] in which the TOCSY spectrum was first used to identify amino acid spin systems, and then the NOESY spectrum was used to make sequential connections between them. Parts A and B of Figure 4 show regions of the NOESY spectrum of the cyclic peptide with the assignments marked. The spectrum of the linear peptide was similar. For the purpose of clarity, the results of 2D NMR spectroscopy are presented by assigning the numbers 1−14 to the peptide sequence CGPEMLNRVSEPGC as indicated in Figure 5.

Inspection of the spectrum in Figure 4A shows a pattern of medium to strong sequential $\alpha(i) - N(i+1)$ cross-peaks, with weaker intraresidue cross-peaks over most residues of the peptide. This is typical of the pattern expected for an extended or random coil conformation, a conclusion that is supported by the observation of weak−medium NH−NH cross-peaks (Figure 4B). The NOE patterns are summarized in Figure 5, together with coupling and chemical shift information. It is noteworthy that there is a weakening of the $\alpha(i) - N(i+1)$ NOEs near residues 6−8 and a strengthening of the corresponding NH−NH cross-peaks. This provides the first indication that among the predominantly random coil conformational ensemble there may be a small population of structured species with local turn-

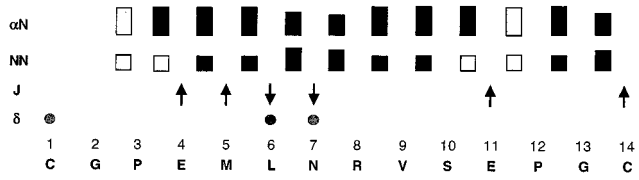

Figure 5. Summary of NMR data used to derive conformational information on ECL3. Sequential and NH−NH NOEs are indicated by filled bars, with the intensity proportional to the height of the bar. Note the weakening of αN and strengthening of NN NOEs near residues 6−8. Shaded bars denote Pro residues (NH signals are absent). Those residues with *J* coupling constants greater than 8 Hz are indicated by up arrows and those less than 5 Hz with down arrows. Residues with αH chemical shifts that deviated from random coil values by more than 0.1 ppm are indicated by filled circles.

like structure near these residues. Chemical shifts and coupling constants of the linear and cyclic peptides were examined to provide support for this suggestion.

Inspection of the derived αH chemical shifts for the backbone protons in the linear peptide showed that they were all within 0.1 ppm of values reported for random coil peptides, apart from the two N-terminal residues. This confirms that the peptide adopts an essentially random coil conformation. Interestingly, however, in the cyclic peptide the chemical shifts for most residues moved slightly away from random coil values, and those for residues L6 and N7 in particular deviated from random coil by more than 0.1 ppm (Figure 5). This indicates that cyclization induces a degree of structuring in the whole peptide but most particularly near the LN dipeptide pair. As indicated above, stronger NH−NH NOEs were detected between these two residues and between N7 and R8. Combined with the observation of a small $^3J_{NH}$ coupling constant (<5 Hz) for N7, this strongly suggests that the cyclic peptide incorporates a turn centered about the residues L, N, and R. The termini of the peptide are linked by a disulfide bond, and their spatial proximity was confirmed by the observation of NOEs, for example, between the αH protons of G2 and the NH of C14, as well as the expected cross-peaks between C1 and C14. The remaining regions of the peptide between the proximate termini and the putative turn at residues 6−8 appear to have an extended conformation for at least some population of the conformational ensemble, judging by the large coupling constants (Figure 5) for some of these residues. The NMR results thus indicate the presence of a small population containing a *β*-hairpin conformation among an ensemble of largely disordered structure.

Raman Spectroscopy. (a) Micro-Raman Spectroscopy. The structure-sensitive, strong amide I band originates mainly from carbonyl C−O stretching vibrations and smaller contributions of coupled vibrations of C−N stretching and N−H in-plane bending. For both ECL3 peptides, in the cyclic and in the linear form, the wavenumbers of the amide I bands are significantly high at 1669 and at 1662 cm^{-1}, respectively (Figure 6). This indicates a low degree of hydrogen bonding typical of unordered structures compared to characteristic wavenumbers around 1645 and 1650 cm^{-1} in helical structures with strong hydrogen bonding.[31] The distinct amide II lines at 1556 and 1553 cm^{-1} appearing in both spectra are noteworthy because they provided further

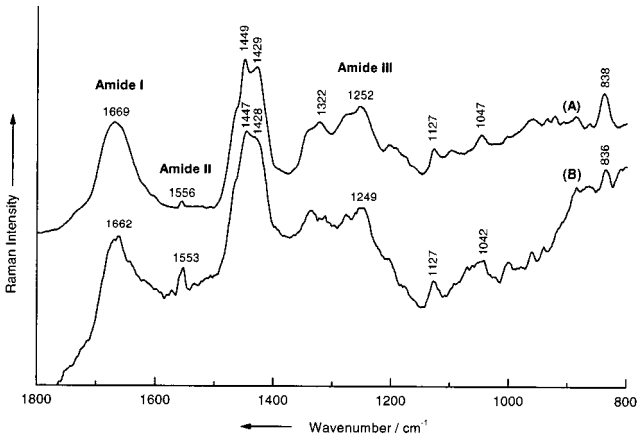

Figure 6. Micro-Raman spectra of ECL3 of mouse GnRH-R (lyophilized sample): (A) cyclic and (B) linear peptides.

Table 1. Wavenumbers (in cm^{-1}) and Raman Cross Sections σ (in mb molecule^{-1} sr^{-1}) of Amide Bands as They Show up in Pure Secondary Structure Raman Component Spectra (Data Taken from Ref 33, Table 3)

	α-helix	σ_α	*β*-sheet	σ_β	unordered	σ_c
amide I	1647	32	1654	48	1665	56
amide II	1545	22	1551	57	1560	71
amide III	1299	24	1235	53	1267	65

information for the Raman band assignment and their structural interpretation. This band was reported to be extremely weak in Raman spectra but quite strong in the corresponding infrared spectrum.[32] The band intensity of an amide band in proteins and peptides is principally governed by the product of the occurrence frequency of the amide bonds and the Raman cross section of the respective band.[33] Table 1 displays the Raman cross sections of *β*-sheet and unordered structures, which appear to be 2.6-fold and 3.2-fold more intense than in α-helix structures. Therefore, from the amide I bands and from the distinct amide II bands in the micro-Raman spectra of both peptides (Figure 6), we concluded the dominance of unordered conformation with partial spectral contributions from the *β*-sheet structure. The typically weak amide II band was also observed in the FT-Raman spectrum of the cyclic ECL3 peptide (Figure 8).

The structure-sensitive amide III band, which originates from significant C−N vibrations coupled with N−H in-plane bending vibrations, appears in the spectral region between 1220 and 1300 cm^{-1}. The amide III band as it appears in the spectra of the various protein conformations (α-helix, *β*-sheet, unordered) has been studied extensively and is considered to be 3 times as sensitive to conformation as the amide I band.[34−38] A summary is listed in Table 1 presenting the wavenumbers of the amide bands I, II, and III as they show up in model compounds with pure secondary structure Raman spectra. In the amide III region of the cyclic form of the ECL3 peptide, a broad band at 1252 cm^{-1} is observed, which can be assigned to unordered structure with some contribution from *β*-sheet conformation (cf. Table 2).

Several characteristic bands in the lower wavenumber region of the Raman spectra are from contributions of bending, twisting, and stretching vibrations from the side chains and (in the cyclic peptide only) from S−S

Table 2. Wavenumbers (in cm^{-1}) and Tentative Assignment for the Observed Lines As Obtained in the Micro-Raman and FT Raman Experiments of ECL3 of Mouse GnRH-R[a]

micro-Raman		LabRam		FT Raman		
ECL3-c	ECL3-l	ECL3-c	ECL3-l	ECL3-c	ECL3-l	assignment
1669 s	1662 s	1666 vs	1668 vs	1666 s	1669 s	amide I
1556 vw	1553 mw			1556 vw		amide II
1449 vs	1447 vs	1445 vs	1445 vs	1449 vs	1449 vs	CH_2 bending
1429 vs	1428 sh	1428 vs	1422 vs		1430 vs	
1322 m		1319 ms	1320 ms			CH_2 twisting
1252 ms	1249 ms	1249 s	1247 s	1246 ms	1254 ms	amide III
1127 ms	1127 ms	1121 m	1121 m	1121 vw	1126 vw	C−N stretching
1047 w	1042 w			1044 mw	1042 mw	CH_2 twist (Pro, Glu, Arg)
838 s	836 s			835 ms	836 ms	Pro
				724 mw	723 mw	Met
				509 ms		S−S stretching

[a] Abbreviations: ECL3-c, cyclic peptide; ECL3-l, linear peptide; s, strong; ms, medium strong; vs, very strong; w weak; mw, medium weak; vw, very weak; sh, shoulder.

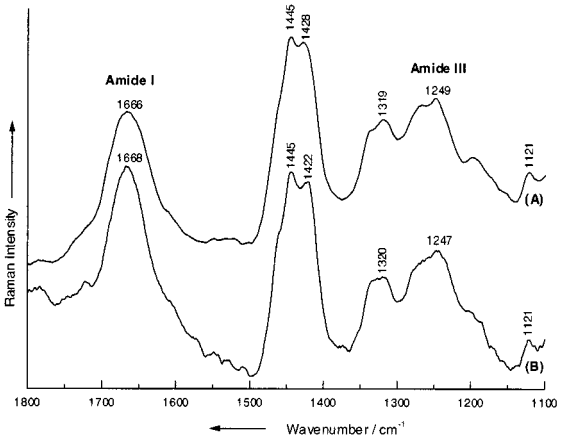

Figure 7. Micro-Raman spectra (LabRam) of ECL3 of mouse GnRH-R (lyophilized sample): (A) cyclic and (B) linear peptides.

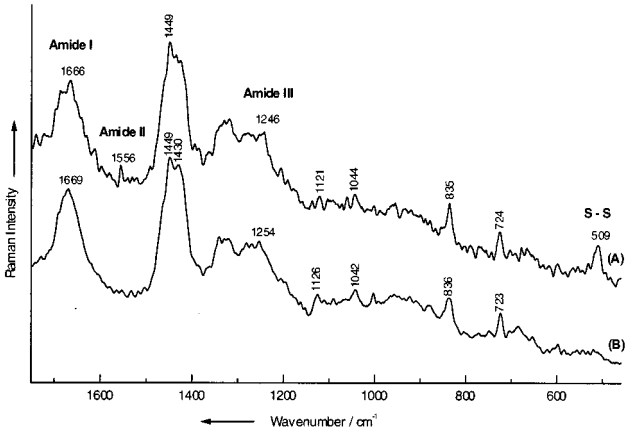

Figure 8. FT Raman spectra of ECL3 of mouse gonadotropin-releasing hormone receptor (lyophilized sample): (A) cyclic and (B) linear peptides.

stretching vibrations. A summary of tentative band assignments is presented in Table 2. The structure-sensitive bands obtained with the LabRam instrument confirmed the results from the micro-Raman experiments (Figure 7). The amide III vibrations were found at 1249 cm^{-1} in the cyclic ECL3 peptide and at 1247 cm^{-1} in the linear ECL3 peptide. This is indicative of the antiparallel band region (1235−1240 cm^{-1}) and the unordered band region (1250−1270 cm^{-1}). The amide III band reported in this study is distinctly different from the typical high amide III band of α-helix assignments.[33] The amide I vibration occurs at 1666 cm^{-1} in the cyclic peptide and at 1668 cm^{-1} in the linear peptide. This clearly reveals that the ECL3 peptides consist predominantly of an unordered structure, and this excludes α-helix conformation (cf. Table 1), which has been reported to appear at a much lower wavenumber of ∼1647 cm^{-1}.[33]

(b) FT Raman Spectroscopy. The lower wavenumber region of the FT-Raman spectra (Figure 8) shows a medium strong line near 836 cm^{-1} assigned to the two Pro residues. The spectral region from 500 to 725 cm^{-1} reveals characteristic bands from the S−S and C−S stretching vibrations. A pronounced line appears at 724 cm^{-1} in the FT-Raman spectrum of the cyclic peptide and at 723 cm^{-1} in the spectrum of the linear peptide. These lines arise from the C−S stretching vibrations of the methionine residue, indicating that in both forms of ECL3 peptides the methionine is in trans conformation.[32] The sharp 509 cm^{-1} line of the cyclic peptide (spectrum A in Figure 8) can be readily assigned to the S−S stretching vibration of the disulfide bridge A compilation, and assignment of these lines is given in Table 2.

Discussion

The interactions between GnRH and its receptor are crucial for normal reproductive function. Studying these interactions is contributing to the design of peptide and non-peptide GnRH analogues, which are extensively used in the treatment of a wide variety of endocrinological and nonendocrinological disorders.[39] Molecular cloning and characterization of GnRH-Rs from a range of vertebrate species have shed light on the nature of the structure−activity relations of the receptor−ligand complex[40] and together with mutagenesis of the receptor have contributed to the refinement of computational molecular models.[2−5,13,14] However, insight into the binding pocket of GnRH is still rudimentary, and its precise interactions need to be defined.

The third extracellular loop has been identified as a microdomain of the binding pocket because it contains an acidic amino acid residue, which has been shown to confer specificity for Arg[8] of GnRH in mouse GnRH-R[18] and in the human GnRH-R.[19] The residues Glu$^{7.32(301)}$ (mouse) and Asp$^{7.32(302)}$ (human) are followed by a Pro in mammalian GnRH-Rs, which have been proposed to play an important role in the orientation of the side

chain of $Glu^{7.32(301)}$/$Asp^{7.32(302)}$ (for details of the receptor numbering scheme, see Figure 1). Possibly this effect is exerted indirectly by influencing the orientation of the acidic residue side chain to interact efficiently with Arg^8 of GnRH [B. Fromme, unpublished results]. The initiation of an α-helix in TM7 in the GnRH-R may be generated by an NP sequence/N-cap motif.[41] In the mammalian GnRH-Rs there are NP and DP (or EP) motifs, which potentially introduce hinges on the N- and C-terminal sides of ECL3 (Figure 1). It has been proposed that ECL3 could exist as an α-helix[42] and that this conformation could also contribute to the presentation of the side chain of the residues $Glu^{7.32(301)}$/$Asp^{7.32(302)}$ in a favorable position for interaction with Arg^8 of GnRH. A series of amino acid substitutions were performed on ECL3 of the human GnRH-R aimed at disrupting the DP cap. These experiments consisted of inserting one to four alanines after P^{294} in ECL3 of human GnRH-R and also of inserting the charged residues E^{295} and R^{299} reciprocally. However, these attempts to disrupt any theoretically predicted structure of the loop did not show expected effects on ligand binding and could not provide an answer as to whether the loop is helical or not [B. Fromme, unpublished results].

The above-mentioned experimental results, which were based on the suggestion of a helically ordered structure in ECL3, have thus prompted us to apply a set of spectroscopic techniques to investigate the secondary structure of synthetic peptides representing the third extracellular loop of GnRH-R. We synthesized a model peptide (CG*PEMLNRVSEP*GC) representing residues 293−302 of mouse ECL3, where Cys and Gly residues are added symmetrically at the N and C termini respectively, allowing the introduction of a disulfide bridge to simulate the distances at which the ECL3 is tethered to the transmembrane domains 6 and 7 of the receptor like the comparable loop in the rhodopsins.[6,7] Both forms of the ECL3 peptides significantly inhibited GnRH stimulation of inositol phosphate production, suggesting that the peptides compete with the receptor loop for binding of GnRH.

In the present study we have shown that Raman spectroscopy, used as a complement to CD and 2D NMR spectroscopy, is a sensitive tool for the conformational analysis of peptides. In particular, the vibrational modes from the CONH groups of the peptide backbone exhibit characteristic Raman bands, which reflect on the peptide conformation. Attention is drawn to the prominent lines around 1660 cm^{-1} (amide I) and in the region of 1220−1300 cm^{-1} (amide III). In the micro-Raman and the FT-Raman spectra, the strong amide I band is observed in the wavenumber region of ∼1669 cm^{-1}. Our analysis of the amide I band in combination with the amide III band shows that the loop does not exhibit any α-helical structure. In addition to these conformational-sensitive lines, the 509 cm^{-1} Raman band gives clear evidence of the presence of the disulfide cross-link in the cyclic form of the ECL3 peptide. This line is absent in the linear form of the peptide. The specificity and reproducibility of the spectral response point to the predominance of an unordered conformation.

The data obtained from CD spectroscopy have confirmed that the synthetic ECL3 peptides, both in the cyclic and in the linear forms, are not helical as has been proposed for the ECL3 receptor domain[42] but rather have an unordered conformation with some minor (not quantified) contributions from β-sheet structure.

The 2D NMR technique, in demonstrating that the linear ECL3 peptide has random coil conformation and no α-helical structure, corroborates the CD and Raman data. However, in the cyclic ECL3 peptide the values of the αH shift from the values of most residues, but those of the central residues L^{296} and N^{297} in particular moved away from the random coil values. Also, from the $^3J_{NH}$ coupling constant for N^{297}, the presence of a β-hairpin with a turn centered on residues L^{296}, N^{297}, and R^{298} was identified among an ensemble of largely disordered structure. From this it is anticipated that the cyclic peptide has a higher tendency to form a β-hairpin (turn) in the central residues (L^{296}, N^{297}, R^{298}) of the loop than the linear analogue. The cyclic model peptide with the disulfide bridge appears suitably designed to mimic the constraints imposed by the connection of TM6 and TM7. Therefore, we suggest that this conformation also exists in the complete native GnRH-R or the receptor loop will have the ability to adopt this conformation.

The structural data concerning the secondary structure of the ECL3 peptides may be compared with 2D NMR studies on the intradiscal loops of rhodopsin, which exhibited a compact structure in solution with turns in the central region of the peptides[8] and of ECL2 in the human thromboxane A_2 receptor[21] that are likewise biologically active. There is increasing evidence that all biologically active loop peptides of GPCRs share a common helix−turn−helix motif.[8] Where helices are observed, they are probably extensions of TM helices. Turns are stabilized by short-range interactions as in β-turns. The primary sequence of the loops is sufficient to code for the turn. Constraining the peptides to this separation by cyclization can mimic structural constraints from the highly ordered TMD structure. These observations strongly support the hypothesis that the tendency of the synthetic ECL3 peptides from the GnRH-R to adopt a loop structure with a β-turn is a reliable indicator of the ability of the loop to assume an active conformation by induction.

The present study demonstrates that the combination of CD, 2D NMR, and Raman spectroscopy exhibits profound potential for the characterization of the structural properties of the receptor and may elucidate the ligand selectivity of ECL3 in binding with Arg^8 of GnRH. We propose that ECL3 of the mammalian GnRH-R exists predominately as a random coil with a central β-hairpin domain and that this conformation may be adequate for the interaction of the acidic residue in ECL3 conferring specificity for Arg^8 in mammalian GnRH.[18,19]

The cyclic ECL3 peptide, which more closely simulates the constraints of the native ECL3, was a slightly more effective inhibitor in the PI hydrolysis assay than the linear peptide. It also differed uniquely from the linear peptide in demonstrating evidence of the β-hairpin conformation. It appears, therefore, that biological activity is correlated with the β-hairpin structure or indirectly with the ability to adopt the β-hairpin structure. Taking reference to the observation that even

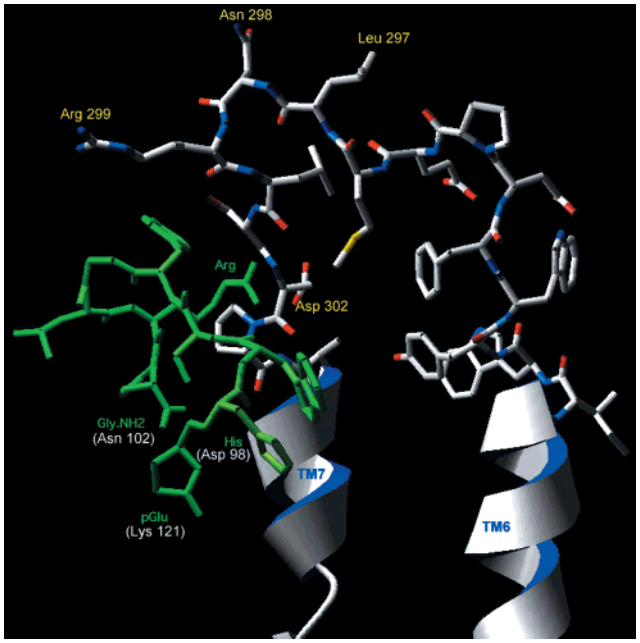

Figure 9. Interaction of Arg^8 in GnRH with Asp^{302} of ECL3 of the human GnRH receptor. The GnRH receptor model was based on the rhodopsin structure and refined to accommodate known experimental data of interactions of TM domains.[2] The β-hairpin conformation of ECL3 determined for the cyclic peptide was attached to TM6 and TM7 of the molecular model. Only TM6, ECL3, and TM7 of the molecular model are shown for clarity. The GnRH molecule in its active β II turned conformation has been docked to the cognate binding sites in the receptor (Asp^{98}, Asn^{102}, Lys^{121}), which are not shown for clarity. With all these contacts in place, Arg^8 of GnRH is able to interact with Asp^{302} of the receptor as shown.

smaller portions of the loops consistently reflect the structure of the larger loops,[8] even the linear ECL3 peptide will have a tendency to adopt a β-turn structure. However, in the linear peptide the fraction, which assumes the hairpin structure, might be below the experimental detection limit of 2D NMR. Nevertheless, the PI assay responds to the ability of the cyclic and the linear peptides to adopt the active conformation. This might explain the small differences between the linear and the cyclic peptides.

We therefore asked the question as to whether the Arg^8 interaction of GnRH with $Glu^{7.32}/Asp^{7.32}$ of ECL3, which is critical for high biological activity, can occur in our molecular model of the GnRH-R. When GnRH was docked to cognate binding sites (Glu^1 to Lys^{121}; His^2 to Asp^{98}; Gly^{10} NH_2 to Asn^{102}),[15−17] the Arg^8 of GnRH was able to interact with Asp^{302} of ECL3 when attached to TM6 and TM7 in the β-hairpin conformation (Figure 9). These findings support the concept that this represents the biologically active conformation.

The structural information obtained in this study contributes to an understanding to what extent the structure or conformation of the third extracellular loop may play a role in receptor binding and activation. Two models have been proposed. In the "conformational induction" model, agonists bind to an inactive receptor state and induce the receptor to assume an altered active state that leads to coupling with G proteins. In the "conformational selection" model, the receptor spontaneously fluctuates between inactive and active conformers, and agonists have a higher affinity for the active state, whereas antagonists have a higher affinity for the inactive state.[2] Agonist binding causes the concentration of active receptor to increase by mass action. In the "conformational induction" model, we have to assume that the first step consists of binding of GnRH to the (inactive) GnRH-R. No assumptions have been made so far about what structural features would be associated with an inactive state. GnRH will then be induced to assume a high-affinity binding conformation by an interaction that involves Arg^8 and $Glu^{7.32}/Asp^{7.32}$ in the receptor.[18,19] To the extent that Arg^8 GnRH and $Glu^{7.32}/Asp^{7.32}$ GnRH-R have a complementary role in defining the high-affinity binding state,[14,18,19] we expect that simultaneously or in an immediately following step the loop domain will assume an "altered" active state represented by a defined structure. In the "conformational selection" model we have to assume that GnRH (the agonist) binds preferentially to a preexisting, active conformation of the receptor. Compared with the induction model, which makes no precise assumptions about the structure of the receptor or the loop domain, in the selection model binding of the ligand requires that part of the receptor (detectably) exists in a predefined structure of the loop domain, which increases by mass action following agonist binding. The proposed stabilization of an induced conformation of ECL3 by the intervention of Arg^8 of the ligand with $Glu^{7.32}/Asp^{7.32}$ of the receptor complements the established induction of a β II turn conformation of the ligand[43,44] by this interaction.[18,19] The β II turn conformation of GnRH is stabilized by Arg^8 and is absent in Gln^8 GnRH.[44,45] Substitution of Gly^6 with a D-amino acid constrains GnRH in the β II turn conformation[2,43,45] and overcomes the 10- to 100-fold decrease in binding affinity resulting from substitution of Arg^8 in GnRH or $Glu^{7.32}/Asp^{7.32}$ in the receptor by neutral amino acids.[18,19] Thus, the interaction of Arg^8 of GnRH with $Glu^{7.32}/Asp^{7.32}$ configures the ligand and is also proposed to configure ECL3 of the receptor.

However, comparable, structurally constrained high-affinity binding state variants of the third loop have not yet been established. Notwithstanding the fact that 2D NMR is considered to provide the most precise structural information from a peptide about the structural organization of a limited size domain, other spectroscopic methods, by which the predominant conformation among an ensemble of conformers can be fast and efficiently documented and which sensitively reflect changes of secondary structure by internal or external signals, appear suitable for tracing conformational changes. In the present paper we have applied CD and Raman spectroscopy as a complement to 2D-NMR spectroscopy, which provides further insight into the structure−function relationship of the extracellular loop of a membrane protein.

Acknowledgment. We are indebted to W. Bouschen, University of Würzburg, for kindly performing mass spectrometric analysis of the peptides. We thank Dr. T. Kortemme, EMBL Heidelberg, for support and for critical discussion of the CD data. We acknowledge in particular P. Taylor for contributing the docking experiments and A. Sheppard for provision of his molecular model of GnRH. The work described in this paper was supported in part by grants from the National

Research Foundation, South Africa (GUN Nos. 2042129 and 2043529), and the Medical Research Councils of South Africa and the United Kingdom and by funds from the Universities of Cape Town and Würzburg. W.K. also thanks the "Fonds der Chemischen Industrie" for financial support. D.J.C. is grateful for the support of an Australian Research Council Senior Fellowship.

References

(1) Fink, G. Gonadotropin secretion and its control. In *The Physiology of Reproduction*; Knobil, E., Neill, J., Eds.; Raven Press: New York, 1988; pp 1349−1377.
(2) Sealfon, S. C.; Weinstein, H.; Millar, R. P. Molecular mechanisms of ligand interaction with the gonadotropin-releasing hormone receptor. *Endocr. Rev.* **1997**, *18*, 180−205.
(3) Baldwin, J. M.; The probable arrangement of the helices in G protein-coupled receptors. *EMBO J.* **1993**, *12*, 1693−1703.
(4) Ballesteros, J. A.; Weinstein, H. Integrated methods for the construction of three-dimensional models and computational probing of structure−function relations in G protein-coupled receptors. *Methods Neurosci.* **1995**, *25*, 366−428.
(5) van Rhee, A. M.; Jacobson, K. A. Molecular architecture of G protein-coupled receptors. *Drug Dev. Res.* **1996**, *37*, 1−38.
(6) Pebay-Peyroula, E.; Rummel, G.; Rosenbusch, J. P.; Landau, E. M. X-ray structure of bacteriorhodopsin at 2.5 angstroms from microcrystals grown in lipidic cubic phases. *Science* **1997**, *277*, 1676−1682.
(7) Palczewski, K.; Kumasaka, T.; Hori, T.; Behnke, C. A.; Motoshima, H.; Fox, B. A.; Le Trong, I.; Teller, D. C.; Okada, T.; Stenkamp, R. E.; Yamamoto, M.; Miyano, M. Crystal structure of rhodopsin: A G protein-coupled receptor. *Science* **2000**, *289*, 739−745.
(8) Yeagle, P. L.; Salloum, A.; Chopra, A.; Bhawsar, N.; Ali, L.; Kuzmanovski, G.; Alderfer, J. L.; Albert, A. D. Structures of the intradiskal loops and amino terminus of the G-protein receptor, rhodopsin. *J. Pept. Res.* **2000**, *55*, 455−465.
(9) Yeagle, P. L.; Alderfer, J. L.; Albert, A. D. Three-dimensional structure of the cytoplasmic face of the G protein receptor rhodopsin. *Biochemistry* **1997**, *32*, 9649−9654.
(10) Yeagle, P. L.; Alderfer, J. L.; Albert, A. D. Structure of the third cytoplasmic loop of bovine rhodopsin. *Biochemistry* **1995**, *34*, 14621−14625.
(11) König, B.; Arendt, A.; McDowell, J. H.; Kahlert, M.; Hargrave, P. A.; Hofmann, K. P. Three cytoplasmic loops of rhodopsin interact with transducin. *Proc. Natl. Acad. Sci. U.S.A.* **1989**, *86*, 6878−6882.
(12) Palm, D.; Münch, G.; Malek, D. Mapping G protein coupling domains by site-specific peptides. *Methods Neurosci.* **1995**, *25*, 302−321.
(13) Gudermann, T.; Schöneberg, T.; Schultz, G. Functional and structural complexity of signal transduction via G-protein-coupled receptors. *Annu. Rev. Neurosci.* **1997**, *20*, 399−427.
(14) Flanagan, C. A.; Millar, R. P.; Illing, N. Advances in understanding gonadotrophin-releasing hormone receptor structure and ligand interactions. *Rev. Reprod.* **1997**, *2*, 113−120.
(15) Davidson, J. S.; McArdle, C. A.; Davies, P.; Elario, R.; Flanagan, C. A.; Millar, R. P. Asn102 of the gonadotropin-releasing hormone receptor is a critical determinant of potency for agonists containing C-terminal glycinamide. *J. Biol. Chem.* **1996**, *271*, 15510−15514.
(16) Flanagan, C. A.; Rodic, V.; Konvicka, K.; Yuen, T.; Chi, L.; Rivier, J. E.; Millar, R. P.; Weinstein, H.; Sealfon, S. C. Multiple interactions of the $Asp^{2.61(98)}$ side chain of the gonadotropin-releasing hormone receptor contribute differentially to ligand interaction. *Biochemistry* **2000**, *39*, 8133−8141.
(17) Zhou, W.; Rodic, V.; Kitanovic, S.; Flanagan, C. A.; Chi, L.; Weinstein, H.; Maayani, S.; Millar, R. P.; Sealfon, S. C. A locus of the gonadotropin-releasing hormone receptor that differentiates agonist and antagonist binding sites. *J. Biol. Chem.* **1995**, *270*, 18853−18857.
(18) Flanagan, C. A.; Becker, I. I.; Davidson, J. S.; Wakefield, I. K.; Zhou, W.; Sealfon, S. C.; Millar, R. P. Glutamate 301 of the mouse gonadotropin-releasing hormone receptor confers specificity for arginine 8 of mammalian gonadotropin-releasing hormone. *J. Biol. Chem.* **1994**, *269*, 22636−22641.
(19) Fromme, B. J.; Katz, A.; Roeske, R. W.; Millar, R. P.; Flanagan, C. A. Role of $aspartate^{7.32(302)}$ of the human gonadotropin-releasing hormone receptor in stabilizing a high affinity ligand conformation. *Mol. Pharmacol.* **2001**, *60*, 1280−1287.
(20) MacArthur, M. W.; Thornton, J. M. Influence of proline residues on protein conformation. *J. Mol. Biol.* **1991**, *218*, 397−412.
(21) Ruan, K.-H.; So, S.-P.; Wu, J.; Li, D.; Huang, A.; Kung, J. Solution structure of the second extracellular loop of human thromboxane A_2 receptor. *Biochemistry* **2001**, *40*, 275−280.
(22) Millar, R. P.; Davidson, J.; Flanagan, C.; Wakefield, I. Ligand binding and second-messenger assays for cloned Gq/G11-coupled neuropeptide receptors: The GnRH receptor. *Methods Neurosci.* **1995**, *25*, 145−162.
(23) Marion, D.; Wüthrich, K. Application of phase sensitive two-dimensional correlated spectroscopy (COSY) for measurements of $^1H-^1H$ spin−spin couplings in proteins. *Biochem. Biophys. Res. Commun.* **1983**, *113*, 967−974.
(24) Rance, M.; Sørensen, O. W.; Bodenhausen, G.; Wagner, G.; Ernst, R. R.; Wüthrich, K. Improved spectral resolution in COSY ^1H NMR spectra of proteins via double quantum filtering. *Biochem. Biophys. Res. Commun.* **1983**, *117*, 479−495.
(25) Braunschweiler, L.; Ernst, R. R. Coherence transfer by isotropic mixing: Application to proton correlation spectroscopy. *J. Magn. Reson.* **1983**, *53*, 521−528.
(26) Bax, A.; Davis, D. G. MLEV-17-based two-dimensional homonuclear magnetization transfer spectroscopy. *J. Magn. Reson.* **1985**, *65*, 355−360.
(27) Jeener, J.; Meier, B. H.; Bachmann, P.; Ernst, R. R. Investigation of exchange processes by two-dimensional NMR spectroscopy. *J. Chem. Phys.* **1979**, *71*, 4546−4553.
(28) Piotto, M.; Saudek, V.; Sklenar, V. Gradient-tailored excitation for single-quantum NMR spectroscopy of aqueous solutions. *J. Biomol. NMR* **1985**, *2*, 661−665.
(29) Brahms, S.; Brahms, J. Determination of protein secondary structure in solution by vacuum ultraviolet circular dichroism. *J. Mol. Biol.* **1980**, *138*, 149−178.
(30) Wüthrich, K. *NMR of Proteins and Nucleic Acids*; John Wiley & Sons Inc.: New York, 1985.
(31) Spiro, Th. G.; Gaber, B. P. Laser Raman scattering as a probe of protein structure. *Annu. Rev. Biochem.* **1977**, *46*, 553−572.
(32) Lord, R. C.; Yu, N.-T. Laser-excited Raman spectroscopy of biomolecules: II. Native ribonuclease and α-chymotrypsin. *J. Mol. Biol.* **1970**, *51*, 203−213.
(33) Chi, Z.; Chen, X. G.; Holtz, J. S. W.; Asher, S. A. UV Resonance Raman-selective amide vibrational enhancement: Quantitative methodology for determining protein secondary structure. *Biochemistry* **1998**, *37*, 2854−2864.
(34) Yu, N.-T.; Liu, C. S.; O'Shea, D. C. Laser Raman spectroscopy and the conformation of insulin and proinsulin. *J. Mol. Biol.* **1972**, *70*, 117−132.
(35) Yu, N.-T.; Jo, B. H. Comparison of protein structure in crystals and in solution by laser Raman scattering. I. Lysozyme. *Arch. Biochem. Biophys.* **1973**, *156*, 469−474.
(36) Yu, N. T.; Jo, B. H. Comparison of protein structure in crystals and in solution by laser Raman scattering. II. Ribonuclease A and carboxypeptidase A. *J. Am. Chem. Soc.* **1973**, *95*, 5033−5037.
(37) Chen, M. C.; Lord, R. C.; Mendelsohn, R. Laser-excited Raman spectroscopy of biomolecules. IV. Thermal denaturation of aqueous lysozyme. *Biochim. Biophys. Acta* **1973**, *328*, 252−260.
(38) Chen, M. C.; Lord, R. C.; Mendelsohn, R. Laser-excited Raman spectroscopy of biomolecules. V. Conformational changes associated with the chemical denaturation of lysozyme. *J. Am. Chem. Soc.* **1974**, *96*, 3038−3042.
(39) Casper, R. F. Clinical uses of gonadotropin-releasing hormone analogues. *Can. Med. Assoc. J.* **1991**, *144*, 153−158.
(40) King, J. A.; Millar, R. P. Evolutionary aspects of gonadotropin-releasing hormone and its receptor. *Cell. Mol. Neurobiol.* **1995**, *15*, 5−23.
(41) Konvicka, K.; Guarnieri, F.; Ballesteros, J. A.; Weinstein, H. A proposed structure for transmembrane segment 7 of G protein-coupled receptors incorporating an Asn-Pro/Asp-Pro motif. *Biophys. J.* **1998**, *75*, 601−611.
(42) Sankararamakrishnan, R.; Konvicka, K.; Mehler, E. L.; Weinstein, H. Solvation in simulated annealing and high-temperature molecular dynamics of proteins: A restrained water droplet model. *Int. J. Quantum Chem.* **2000**, *77*, 174−186.
(43) Karten, M. J.; Rivier, J. E. M. Gonadotropin-releasing hormone analogue design. Structure−function studies toward the development of agonists and antagonists: Rationale and perspective. *Endocr. Rev.* **1986**, *7*, 44−66.
(44) Guarnieri, F.; Weinstein, H. Conformational memories and the exploration of biologically relevant peptide conformations: An illustration for the gonadotropin-releasing hormone. *J. Am. Chem. Soc.* **1996**, *118*, 5580−5589.
(45) de L. Milton, R. C.; King, J. A.; Badminton, M. N.; Tobler, C. J.; Lindsey, G. G.; Fridkin, M.; Millar, R. P. Comparative structure−activity studies on mammalian $[Arg^8]$ LH−RH and chicken $[Gln^8]$ LH−RH by fluorimetric titration. *Biochem. Biophys. Res. Commun.* **1983**, *111*, 1082−1088.

JM011036K